


Breakdown of Detailed Balance for Thermal Radiation by Synthetic Fields

S.-A. Biehs^{*}

*Institut für Physik, Carl von Ossietzky Universität, D-26111 Oldenburg, Germany
and Center for Nanoscale Dynamics (CeNaD), Carl von Ossietzky Universität, 26129 Oldenburg, Germany*

G. S. Agarwal[†]

*Institute for Quantum Science and Engineering and Department of Biological and
Agricultural Engineering Department of Physics and Astronomy, Texas A&M University, College Station, Texas 77845, USA*

 (Received 18 October 2022; revised 8 January 2023; accepted 21 February 2023; published 13 March 2023)

In recent times the possibility of nonreciprocity in heat transfer between two bodies has been extensively studied. In particular the role of strong magnetic fields has been investigated. A much simpler approach with considerable flexibility would be to consider heat transfer in synthetic electric and magnetic fields that are easily applied. We demonstrate the breakdown of detailed balance for the heat transfer function $\mathcal{T}(\omega)$, i.e., the spectrum of heat transfer between two objects due to the presence of synthetic electric and magnetic fields. The spectral measurements carry much more physical information and are the reason for the quantum theory of radiation. We demonstrate explicitly the synthetic field induced nonreciprocity in the heat transfer transmission function between two graphene flakes and for the Casimir coupling between two objects. Unlike many other cases of heat transfer, the latter case has interesting features of the strong coupling. Further the presence of synthetic fields affects the mean occupation numbers of two membranes and we propose this system for the experimental verification of the breakdown of detailed balance.

DOI: [10.1103/PhysRevLett.130.110401](https://doi.org/10.1103/PhysRevLett.130.110401)

Reciprocity and detailed balance are at the heart of Kirchhoff's law stating that the absorptivity equals emissivity for any frequency and angle of incidence. In fact, the second law of thermodynamics enforces the reciprocity or better detailed balance of the radiative heat transfer between two objects. Here, it is unimportant if far-field heat transfer is considered where Planck's blackbody determines the upper limit or near-field heat transfer where the blackbody limit is not a limit anymore [1–3] as experimentally tested by a great number of experiments [4–12] within the last decade. How the second law enforces detailed balance can be understood [13] by considering the heat flux between two objects by first taking the transferred power from object a to object b given by

$$P_{a \rightarrow b} = \int_0^\infty \frac{d\omega}{2\pi} \hbar \omega n_a(\omega) \mathcal{T}_{ab}(\omega), \quad (1)$$

where \hbar is the Planck constant, $n_a(\omega) = (\exp(\hbar\omega/k_B T_a) - 1)^{-1}$ is the photonic occupation number, k_B is the Boltzmann constant, and T_a is the temperature of object a . The quantity $\mathcal{T}_{ab}(\omega)$ is a heat transfer function (HTF) for the heat flow from object a to object b . Similarly, the heat flow from object b to object a is given by

$$P_{b \rightarrow a} = \int_0^\infty \frac{d\omega}{2\pi} \hbar \omega n_b(\omega) \mathcal{T}_{ba}(\omega), \quad (2)$$

with $n_b(\omega) = (\exp(\hbar\omega/k_B T_b) - 1)^{-1}$ and T_b the temperature of object b . In thermal equilibrium the objects have the

same temperature $T_a = T_b$ and therefore there is no net heat flow, which means that $P_{a \rightarrow b} = P_{b \rightarrow a}$ and hence

$$\int_0^\infty \frac{d\omega}{2\pi} \hbar \omega n_a(\omega) [\mathcal{T}_{ba}(\omega) - \mathcal{T}_{ab}(\omega)] = 0. \quad (3)$$

Since this expression holds for any value of temperature $T_a = T_b$ and therefore for different spectral weighting by n_a it can be concluded that the validity of the second law of thermodynamics is equivalent to the relation $\mathcal{T}_{ab}(\omega) = \mathcal{T}_{ba}(\omega)$ regardless of any symmetry [14]. That means that even when time reversal symmetry is broken by applying a magnetic field or using topological Weyl semimetals, for instance, detailed balance of the energy HTF must be fulfilled. However, in nonreciprocal systems the detailed balance of thermal radiation can be nearly completely violated when considering three objects [15], which also offers applications for optimized nonreciprocal thermophotovoltaic energy conversion [16]. Similarly, the HTFs do not need to fulfill $\mathcal{T}_{ab}(\omega) = \mathcal{T}_{ba}(\omega)$ when at least a third object c or a nonreciprocal environment are present. In such systems of at least three bodies or two bodies with a nonreciprocal environment one can have $\mathcal{T}_{ab}(\omega) \neq \mathcal{T}_{ba}(\omega)$ and therefore several interesting effects for thermal radiation in general and radiative heat exchange in nanoparticle systems [3] in particular such as persistent heat currents and heat fluxes [17–19], persistent spin and angular momenta [18–20], giant thermal resistance [13,21], a normal and anomalous Hall effect for thermal radiation [22–24], as

well as a diode effect with nonreciprocal surface waves [25]. In all these studied systems, in order to realize a nonreciprocal heat flux or a violation of detailed balance the presence of a third body seems to be a necessary condition. However, within the framework of fluctuational electrodynamics and the scattering formalism [26,27] a formal proof detailed in Ref. [28] shows that $\mathcal{T}_{ab}(\omega) = \mathcal{T}_{ba}(\omega)$ if the environment and the objects both fulfill Lorentz reciprocity [29]. Therefore, in principle for radiative heat transfer between two objects with nonreciprocal properties in a reciprocal environment detailed balance can be broken even though in practice this has not been observed so far.

Interestingly, the presence of synthetic electric and magnetic fields offers the possibility to break the detailed balance of energy transmission functions even for only two coupled resonators, which results in a nonreciprocal energy transmission as shown theoretically and verified experimentally [30]. The synthetic fields are generated by external modulation of the resonance frequency of the two resonators, which first of all generates sidebands that can be understood by the presence of a synthetic electric field in the synthetic frequency domain [31]. When the modulation of the two resonators is phase-shifted, a synthetic magnetic field for the photons is generated [32], which enables the Aharonov-Bohm effect for photons [33], for instance. Now, dynamic modulations of temperatures, material properties, and the coupling strength between the objects have also been considered for modulation of radiative heat exchange between two or more objects [34–37] showing that the modulation of the temperature or chemical potential can result in a shuttling effect [38] and the modulation of material properties can be used to modulate the radiative heat flux between two or more objects [39,40]. Furthermore the modulation of the coupling strength along with engineering of the thermal reservoir allows for nonreciprocal heat transfer in a three-body configuration [41].

In this Letter, by using a quantum Langevin equation approach to treat heat transfer we show that synthetic fields can lead to a breakdown of detailed balance for the HTF between two resonant objects, i.e., we explicitly show that $\mathcal{T}_{ab}(\omega) \neq \mathcal{T}_{ba}(\omega)$. We further show that this broken detailed balance does not result in a nonreciprocal heat flux, i.e., we still have $P_{a \rightarrow b} = P_{b \rightarrow a}$ and the validity of Eq. (3). We will discuss these features for the radiative heat flux between two graphene flakes in which case the synthetic fields are realized by modulating Fermi energies. Furthermore, we propose to measure the broken detailed balance in the strong-coupling regime of two Casimir-force coupled membranes as used in recent experiments like in Ref. [42].

In the following, we describe the near-field radiative heat flux between two graphene flakes as well as Casimir-force coupled membranes by two coupled oscillators [43–46]. The oscillator frequencies $\omega_{a/b}$ then correspond to the frequencies of the main optical or vibrational modes of the graphene flakes or the membranes and their damping is

described by the damping constants $\kappa_{a/b}$. The coupling strength between the oscillators g quantifies the interaction strength of the graphene flakes or membranes due to the fluctuational electromagnetic fields that are at the origin of the radiative heat transfer and Casimir force. Then the coupled oscillators can be described by a set of two quantum Langevin equations [47,48]

$$\dot{a} = -i\omega_a a - \kappa_a a - igb + F_a, \quad (4)$$

$$\dot{b} = -i\omega_b b - \kappa_b b - iga + F_b \quad (5)$$

for the lowering operators a and b of the two coupled oscillators. Furthermore, both oscillators are assumed to be coupled to their own baths that enter here through the bath operators $F_{a/b}$ into the description.

Now, we introduce synthetic electric and magnetic fields via the identical frequency modulation of both oscillators

$$\omega_a \rightarrow \omega_a + \beta \cos(\Omega t) \quad \text{and} \quad \omega_b \rightarrow \omega_b + \beta \cos(\Omega t + \theta) \quad (6)$$

with modulation frequency Ω , amplitude β , and with a phase shift θ . By Fourier transforming the coupled Langevin equations into frequency space we obtain the set of equations in the compact form

$$\boldsymbol{\psi} = \mathbb{M}\boldsymbol{F} + \frac{\beta}{2i}\mathbb{M}\mathbb{Q}_+\boldsymbol{\psi}_+ + \frac{\beta}{2i}\mathbb{M}\mathbb{Q}_-\boldsymbol{\psi}_- \quad (7)$$

by introducing the vectors $\boldsymbol{\psi} = (a(\omega), b(\omega))^t$, $\boldsymbol{\psi}_\pm = (a(\omega \pm \Omega), b(\omega \pm \Omega))^t$, and $\boldsymbol{F} = (F_a(\omega), F_b(\omega))^t$, and the matrices

$$\mathbb{M} = \mathbb{A}^{-1} \quad \text{with} \quad \mathbb{A} = \begin{pmatrix} X_a & ig \\ ig & X_b \end{pmatrix} \quad (8)$$

so that

$$\mathbb{M} = \frac{1}{X_a X_b + g^2} \begin{pmatrix} X_b & -ig \\ -ig & X_a \end{pmatrix} \quad (9)$$

introducing $X_{a/b} = -i(\omega - \omega_{a/b}) + \kappa_{a/b}$ and the diagonal matrix $\mathbb{Q}_\pm = \text{diag}(1, e^{\pm i\theta})$. This compact form makes obvious that we have an infinite set of equations in frequency space due to the coupling to the sidebands $\pm\Omega$, $\pm 2\Omega$, etc., introduced by the modulation. These sidebands can be understood as generated by an electric synthetic field along the synthetic frequency axis (see Fig. 1). Furthermore, the phase shift itself can be interpreted by a synthetic magnetic field [30] that adds a phase \mathbb{Q}_+ for “upward” and \mathbb{Q}_- for “downward” transitions in the frequency bands. Recently, it has been shown theoretically and experimentally that this synthetic magnetic field results

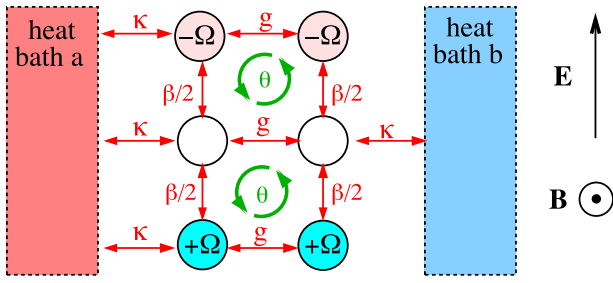


FIG. 1. Sketch of the forward heat flux $P_{a \rightarrow b}$ in the considered two couples oscillators with periodic modulation in the synthetic dimension with the synthetic electric and magnetic fields E and B .

in nonreciprocal energy transmission in coupled oscillator systems [30]. From the mathematical expression of Q_{\pm} it is clear that $Q_{+} = Q_{-}$ for phases $\theta = l\pi$ for all integers l . Hence, for such phases the synthetic magnetic field makes no difference for “upward” and “downward” transitions and we can expect that there is no breaking of detailed balance by the synthetic magnetic field.

Furthermore, the compact matrix form allows us to write down formally the infinite set of equations in frequency space. To this end, we introduce the infinitely large block vectors

$$\underline{\Psi} = (\dots, \Psi_{++}, \Psi_{+}, \Psi, \Psi_{-}, \Psi_{--}, \dots)^t \quad (10)$$

$$\underline{F} = (\dots, F_{++}, F_{+}, F, F_{-}, F_{--}, \dots)^t, \quad (11)$$

where the indices are defined as $F_{\pm} = (F_a(\omega \pm \Omega), F_b(\omega \pm \Omega))^t$, $F_{++/--} = (F_a(\omega \pm 2\Omega), F_b(\omega \pm 2\Omega))^t$, etc. Then we can rewrite the coupled Langevin Eq. (7) as

$$\underline{\Psi} = \underline{\mathbb{L}}^{-1} \underline{\mathbb{M}} \underline{F}, \quad (12)$$

where the diagonal and tridiagonal block matrices $\underline{\mathbb{M}}$ and $\underline{\mathbb{L}}$ are defined in the Supplemental Material [48]. For any solution of this matrix equation it is necessary to consider only a finite subset. As typically done in such a Floquet-Shirley type approach we consider only block vectors of size $2(2N + 1)$ with the corresponding block matrices of size $2(2N + 1) \times 2(2N + 1)$ centered around the solution for the zeroth sideband. The result can be considered as a perturbation result up to order N .

Finally, we can derive a general expression for the spectral correlation functions $\langle a^{\dagger} a \rangle_{\omega}$, $\langle b^{\dagger} b \rangle_{\omega}$, $\langle a^{\dagger} b \rangle_{\omega}$, and $\langle b^{\dagger} a \rangle_{\omega}$. To this end, we first separate the contributions to $\underline{\Psi}$ due to the bath operator \underline{F}_a and \underline{F}_b by introducing the two block matrices $\underline{\mathbb{Y}}_a = \text{diag}(1, 0, 1, 0, \dots)$ and $\underline{\mathbb{Y}}_b = \text{diag}(0, 1, 0, 1, \dots)$ so that $\underline{\mathbb{Y}}_a + \underline{\mathbb{Y}}_b = \underline{\mathbb{1}}$. These two matrices allow us to split the contributions from bath a and bath b so that we obtain

$$\underline{\Psi} = \underline{\mathbb{L}}^{-1} \underline{\mathbb{M}} \underline{\mathbb{Y}}_a \underline{F} + \underline{\mathbb{L}}^{-1} \underline{\mathbb{M}} \underline{\mathbb{Y}}_b \underline{F}. \quad (13)$$

We assume that the bath operators fulfill the fluctuation-dissipation theorem in the form ($i, j = a, b$)

$$\langle F_i^{\dagger}(\omega + l\Omega) F_j(\omega' + l'\Omega) \rangle = \delta_{i,j} \delta_{l,l'} 2\pi \delta(\omega - \omega') \langle F_i^{\dagger} F_i \rangle_{\omega}, \quad (14)$$

with $\langle F_a^{\dagger} F_a \rangle_{\omega} = 2\kappa_a n_a(\omega_a)$ and $\langle F_b^{\dagger} F_b \rangle_{\omega} = 2\kappa_b n_b(\omega_b)$. This assumption can be made as long as the modulation frequencies Ω are much smaller than the inverse coherence time of the bath $k_B T / \hbar$ and the modulation amplitudes β are much smaller than the main resonance frequencies $\omega_{a/b}$. These assumptions are valid in a realistic range of modulation frequencies and amplitudes. For a more general approach covering also higher modulation frequencies and amplitudes the white noise assumption must be relaxed and in the above equation $\langle F_i^{\dagger} F_i \rangle_{\omega}$ must be replaced by $\langle F_i^{\dagger} F_i \rangle_{\omega + l\Omega}$ as detailed in Sec. X of the Supplemental Material [48]. Therewith we arrive at the final result

$$\langle \underline{\Psi}_a^{\dagger} \underline{\Psi}_b \rangle_{\omega} = \sum_{j=a,b} 2\kappa_j n_j(\omega_j) (\underline{\mathbb{L}}^{-1} \underline{\mathbb{M}} \underline{\mathbb{Y}}_j \underline{\mathbb{M}}^{\dagger} \underline{\mathbb{L}}^{-1 \dagger})_{\beta, \alpha} \quad (15)$$

using the properties $\underline{\mathbb{Y}}_{a/b}^{\dagger} = \underline{\mathbb{Y}}_{a/b}$ and $\underline{\mathbb{Y}}_{a/b} \underline{\mathbb{Y}}_{a/b} = \underline{\mathbb{Y}}_{a/b}$. From this expression we can numerically calculate all spectral correlation functions. For instance $\langle a^{\dagger} a \rangle_{\omega}$ is given by the component $\alpha = 2N + 1$ and $\beta = 2N + 1$, $\langle a^{\dagger} b \rangle_{\omega}$ by the component $\alpha = 2N + 1$ and $\beta = 2N + 2$, etc. Note, that due to the white noise assumption the such obtained spectral correlation functions are the sum of all sideband frequency components with equal weighting factors $2\kappa_a n_a$ and $2\kappa_b n_b$.

Let us now use the model to discuss the heat flux between two graphene flakes. Graphene flakes have sharp resonances like plasmonic nanoparticles. The permittivity of a graphene flake lying within a plane parallel to the x - y plane is given by the polarizability tensor $\underline{\alpha} = \text{diag}(\alpha, \alpha, 0)$ with [49]

$$\alpha = \frac{3c^3 k_r}{2\omega_p^2} \frac{1}{\omega_p^2 - \omega^2 - ik\omega} \quad (16)$$

with plasma frequency ω_p , amplitude k_r , and damping constant k , which depend on the Fermi level E_F (in eV) [48] and can be changed by electrical gating, for instance, so that a modulation of the resonance frequency on the order of hundreds of kHz with a change in Fermi level of 0.09 eV are already experimentally feasible [37,50]. Higher modulation frequencies might be achievable with laser pumping methods [51]. The HTF between two identical graphene flakes facing each other at a distance d is within fluctuational electrodynamics in the quasistatic regime given by [48]

$$\mathcal{T}_{ab}(\omega) = \mathcal{T}_{ba}(\omega) = 8 \frac{(\alpha'')^2}{(4\pi d^3)^2} \frac{1}{|1 + \frac{\alpha^2}{(4\pi d^3)^2}|^2}. \quad (17)$$

This HTF can now be related to our model. Within our model, by setting $F_b = 0$ the steady state power from a to b is [48]

$$P_{a \rightarrow b} = \int_0^\infty \frac{d\omega}{2\pi} \hbar \omega_a 2\kappa_a \langle b^\dagger b \rangle_\omega \quad (18)$$

so that the HTF is

$$\mathcal{T}_{ab} = \frac{2\kappa_a}{n_a(\omega_a)} \langle b^\dagger b \rangle_\omega. \quad (19)$$

Similarly, \mathcal{T}_{ba} can be obtained by exchanging a and b . Without any modulation we can directly determine the HTF from Eq. (7) for $\beta = 0$ and $F_b = 0$. Then we obtain [48]

$$\mathcal{T}_{ab} = \frac{4(g\kappa_a)^2}{|X_a^2 + g^2|^2}. \quad (20)$$

By identifying the resonance frequency $\omega_a = \omega_b$ with the plasma frequency ω_p and $\kappa_a = \kappa_b \equiv \kappa$ with damping constant k of the graphene sheet we can fit the HTF of our model to that of Eq. (17). We obtain a very good spectral fit for $g = 0.011\kappa_a$ for $d = 100$ nm (see Supplemental Material [48]).

In Fig. 2 we show the numerical results for the HTF for two identical graphene sheets with $\omega_a = \omega_b = \omega_p = 1.69 \times 10^{14}$ rad/s and $\kappa_a = \kappa_b = 0.013 \omega_p$ for $E_F = 0.4$ eV when the resonance frequencies are modulated as in Eq. (6). Corresponding to the limits of our model, we choose a relatively small amplitude $\beta = 0.05 \omega_p$ that approximately corresponds to a change of the Fermi energy by 0.05 eV and a relatively small modulation frequency $\Omega = 0.05 \omega_p$. First of all it can be seen that as expected the modulation produces sidebands around the resonance frequency ω_p . More interesting is that the spectra are in general different for $\theta \neq l\pi$ ($l \in \mathbb{Z}$) so that the detailed balance between the HTF is broken and we clearly have $\mathcal{T}_{ab}(\omega) \neq \mathcal{T}_{ba}(\omega)$, which is due to the synthetic electric and magnetic fields. However, the integrated heat flux shown in Fig. 3 is reciprocal so that we find $P_{a \rightarrow b} = P_{b \rightarrow a}$, which is in full agreement with the general statement in Eq. (3). An analytical proof of $P_{a \rightarrow b} = P_{b \rightarrow a}$ in presence of synthetic fields can be found in Sec. VII of the Supplemental Material [48]. The modulation generates, in general, a work rate that will result in an energy flow even for $T_a = T_b$. Nonetheless, in our model this energy flow is not accounted for due to the virtue of the white noise assumption. Hence, our model naturally restricts itself to the heat flow in the system. Another feature is that the heat flux can be inhibited due to the modulation, which can be

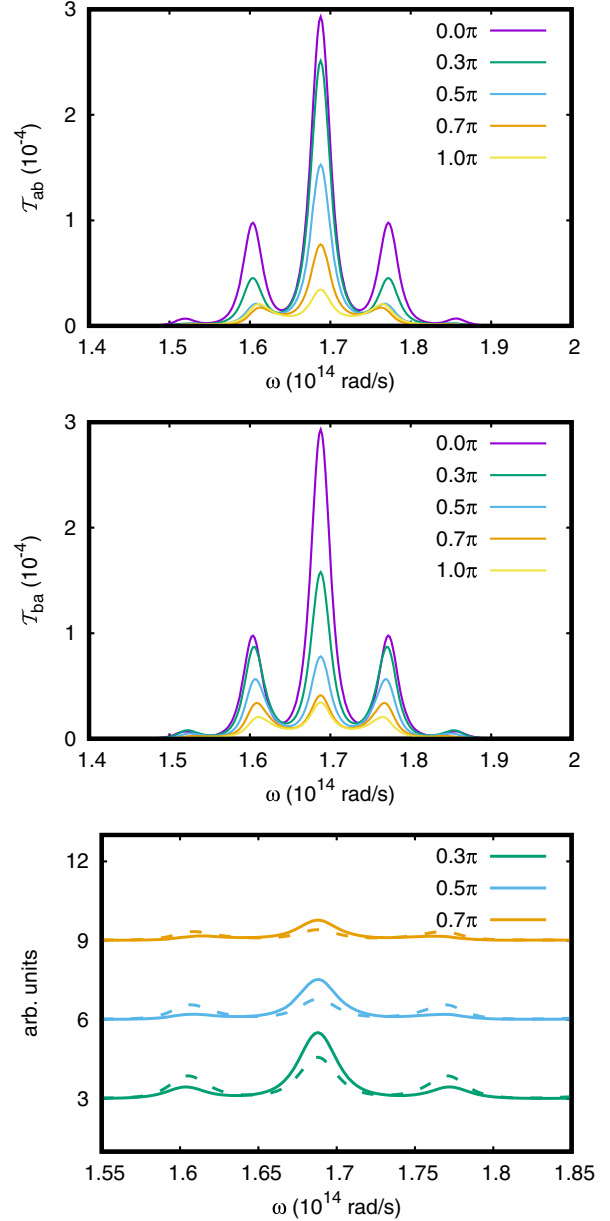


FIG. 2. Nonreciprocal HTF $\mathcal{T}_{ab/ba}$ for graphene flakes at distance $d = 100$ nm using perturbation order $N = 20$. Top: \mathcal{T}_{ab} for $n_a \neq 0$ and $n_b = 0$. Middle: \mathcal{T}_{ba} for $n_b \neq 0$ and $n_a = 0$. Parameters: $\beta = 0.05 \omega_p$, $\Omega = 0.05 \omega_p$, and θ is varied. Bottom: \mathcal{T}_{ab} (full lines) and \mathcal{T}_{ba} (dashed lines) for $\theta = 0.3\pi$, 0.5π , 0.7π with zero lines shifted to 3, 6, 9, respectively.

easily understood by the fact that the resonances do less overlap during a modulation cycle when they are phase shifted. It is an interesting feature that this inhibition can be extremely high for specific combinations of Ω and β ; in particular for $\beta \approx \Omega$ the heat flux can be up to 300 times smaller than without modulation for moderate values of modulation frequencies and amplitudes.

Next, we consider a system of two membranes coupled by Casimir forces that allow for measurements of the spectra of the mean occupation numbers $\langle a^\dagger a \rangle_\omega$ and $\langle b^\dagger b \rangle_\omega$

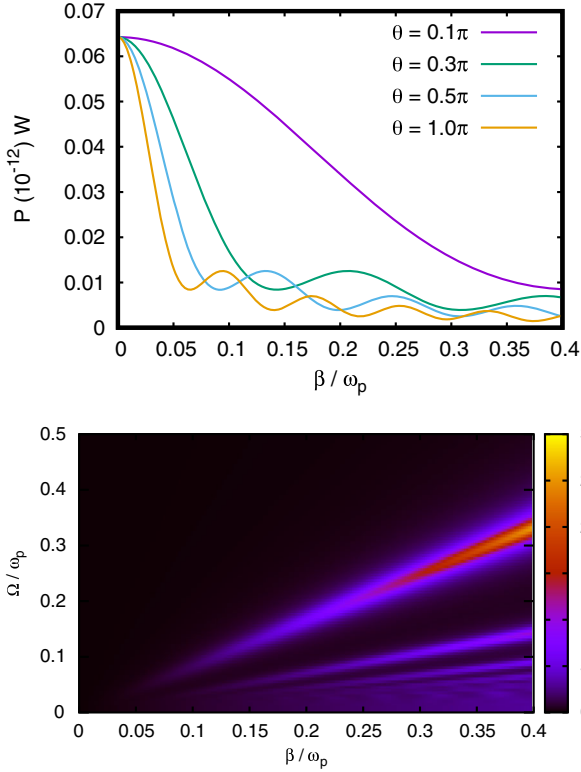


FIG. 3. Top: Total heat flux $P_{a \rightarrow b}$ between two graphene flakes at distance $d = 100$ nm ($g/\kappa = 3.9$) for $T_a = 300$ K and $T_b = 0$ K as function of the modulation amplitude β using dephasings $\theta = 0.1\pi, 0.3\pi, 0.5\pi, 1.0\pi$. Bottom: $P_0/P_{a \rightarrow b}$ as function of β and Ω where P_0 is the value without modulation for $\theta = 1.0\pi$. Numerical calculation is done for $N = 20$.

of the membranes as done in Ref. [42], for instance. In that work the parameters are given by $\kappa_a = \omega_a/(2Q_a)$ and $\kappa_b = \omega_b/(2Q_b)$ for the damping with oscillation frequencies $\omega_a = \omega_b = 2\pi \cdot 191.6$ kHz $\equiv \omega_0$ and quality factors $Q_a = 4.5 \times 10^4$ and $Q_b = 2 \times 10^4$. For an unambiguous identification of the impact of the synthetic fields we choose $\kappa_a = \kappa_b = 10\omega_a/(2Q_a) \equiv \kappa$, which is much larger than in the actual experiment. The coupling constant due to the Casimir force is $g(d) = d^{-4.912} \times 10^{-30}$ s $^{-1}$. The measurements were carried out for distances from $d = 300$ nm, which is in the strong-coupling regime ($g/\kappa = 1.54$), to $d = 800$ nm in the weak-coupling regime ($g/\kappa_1 = 0.013$). The transition between both regimes ($g/\kappa = 1$) occurs at a distance of about 330 nm. A modulation of the membranes might be realized by using stress-controlled piezoelectric actuation as in Ref. [52] where modulation amplitudes of $\beta \approx 0.001 \omega_0$ were achieved and modulation frequencies in the MHz regime can be expected.

In Fig. 4, we show the HTFs \mathcal{T}_{ab} and \mathcal{T}_{ba} in the strong-coupling regime. The broken detailed balance in the strong coupling can be nicely seen. For an experimental verification a measurement of the mean occupation numbers as done in Ref. [42] can be made that show imbalances

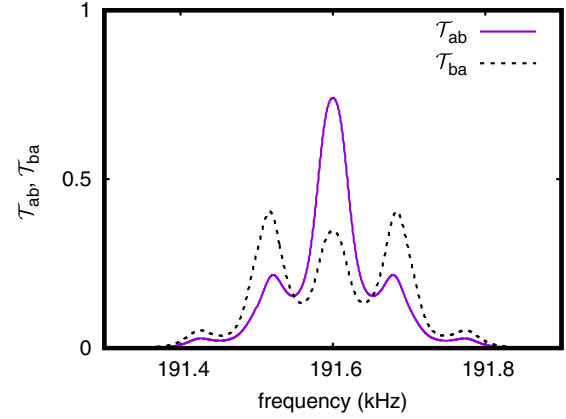


FIG. 4. HTFs \mathcal{T}_{ab} (full lines) and \mathcal{T}_{ba} (dashed lines) of two coupled membranes in strong-coupling regime with $d = 300$ nm with modulation parameters $\Omega = 0.0005 \omega_0$, $\beta = 0.0005 \omega_0$, and $\theta = \pi/2$. Numerical calculation is done for $N = 10$.

directly connected with the broken detailed balance (see Figs. 3 and 4 in the Supplemental Material [48]). However, when assuming that $n_a = n_b$ we find that $\langle a^\dagger a \rangle/n_a + \langle a^\dagger a \rangle/n_b$ equals exactly $\langle b^\dagger b \rangle/n_a + \langle b^\dagger b \rangle/n_b$. Hence, in global equilibrium the synthetic field has no impact on the total occupation numbers of the membranes, which coincides with the result that the heat flux is reciprocal, i.e., $P_{a \rightarrow b} = P_{b \rightarrow a}$. Therefore, the impact of the synthetic fields can only be measured when both membranes have different temperatures as realized in Ref. [42]. It has to be emphasized that the broken detailed balance due to the synthetic fields as seen in the imbalance of the occupation numbers becomes prominent in strong-coupling regime as discussed in greater detail in Sec. IX of the Supplemental Material [48].

In conclusion, we have shown that the presence of electric and magnetic synthetic fields breaks the detailed balance of the HTF but without resulting in a nonreciprocal total heat flux between two objects. We have discussed this phenomenon for the near-field radiative heat transfer between two graphene flakes. Furthermore we could show that synthetic fields allow for a strong heat flux inhibition that can be used to thermally isolate the graphene flakes by periodic modulations. Finally, we propose to measure the breakdown of detailed balance by measuring the mean occupation numbers of Casimir-forced coupled membranes having different temperatures as recently done without dynamic modulation.

S.-A. B. acknowledges helpful discussions with Philippe Ben-Abdallah and support from Heisenberg Programme of the Deutsche Forschungsgemeinschaft (DFG, German Research Foundation) under the Project no. 461632548. This research was supported in part by the National Science Foundation under Grant No. NSF PHY-1748958. G. S. A. thanks the kind support of the Air Force Office of Scientific

Research (AFOSR Award No. FA9550-20-1-0366), The Robert A. Welch Foundation (Grant No. A-1943), and the Infosys Foundation Chair of the Department of Physics, IISc Bangalore.

*Corresponding author.

s.age.biehs@uni-oldenburg.de

†Corresponding author.

girish.agarwal@tamu.edu

- [1] J. C. Cuevas and F. J. Garcia-Vidal, *ACS Photonics* **5**, 3896 (2018).
- [2] P. S. Venkataram, S. Molesky, W. Jin, and A. W. Rodriguez, *Phys. Rev. Lett.* **124**, 013904 (2020).
- [3] S.-A. Biehs, R. Messina, P. S. Venkataram, A. W. Rodriguez, J. C. Cuevas, and P. Ben-Abdallah, *Rev. Mod. Phys.* **93**, 025009 (2021).
- [4] L. Hu, A. Narayanaswamy, X. Chen, and G. Chen, *Appl. Phys. Lett.* **92**, 133106 (2008).
- [5] R. S. Ottens, V. Quetschke, S. Wise, A. A. Alemi, R. Lundock, G. Mueller, D. H. Reitze, D. B. Tanner, and B. F. Whiting, *Phys. Rev. Lett.* **107**, 014301 (2011).
- [6] T. Kralik, P. Hanzelka, M. Zobac, V. Musilova, T. Fort, and M. Horak, *Phys. Rev. Lett.* **109**, 224302 (2012).
- [7] M. Lim, S. S. Lee, and B. J. Lee, *Phys. Rev. B* **91**, 195136 (2015).
- [8] J. I. Watjen, B. Zhao, and Z. M. Zhang, *Appl. Phys. Lett.* **109**, 203112 (2016).
- [9] M. P. Bernardi, D. Milovich, and M. Francoeur, *Nat. Commun.* **7**, 12900 (2016).
- [10] B. Song, D. Thompson, A. Fiorino, Y. Ganjeh, P. Reddy, and E. Meyhofer, *Nat. Nanotechnol.* **11**, 509 (2016).
- [11] A. Fiorino, D. Thompson, L. Zhu, R. Mittapally, S.-A. Biehs, O. Bezencenet, N. El-Bondry, S. Bansropun, P. Ben-Abdallah, E. Meyhofer, and P. Reddy, *ACS Nano* **12**, 5774 (2018).
- [12] A. Fiorino, D. Thompson, L. Zhu, B. Song, P. Reddy, and E. Meyhofer, *Nano Lett.* **18**, 3711 (2018).
- [13] I. Latella and P. Ben-Abdallah, *Phys. Rev. Lett.* **118**, 173902 (2017).
- [14] C. Guo and S. Fan, *Phys. Rev. B* **102**, 085401 (2020).
- [15] L. Zhu and S. Fan, *Phys. Rev. B* **90**, 220301(R) (2014).
- [16] Y. B. Park, B. Zhao, and S. H. Fan, *Nano Lett.* **22**, 448 (2022).
- [17] L. Zhu and S. Fan, *Phys. Rev. Lett.* **117**, 134303 (2016).
- [18] M. G. Silveirinha, *Phys. Rev. B* **95**, 115103 (2017).
- [19] A. Ott, P. Ben-Abdallah, and S.-A. Biehs, *Phys. Rev. B* **97**, 205414 (2018).
- [20] C. Khandekar and Z. Jacob, *New J. Phys.* **21**, 103030 (2019).
- [21] M.-J. He, H. Qi, Y.-X. Su, Y.-T. Ren, Y.-J. Zhao, and M. Antezza, *Appl. Phys. Lett.* **117**, 113104 (2020).
- [22] P. Ben-Abdallah, *Phys. Rev. Lett.* **116**, 084301 (2016).
- [23] A. Ott, R. Messina, P. Ben-Abdallah, and S.-A. Biehs, *J. Photonics Energy* **9**, 032711 (2019).
- [24] A. Ott, S.-A. Biehs, and P. Ben-Abdallah, *Phys. Rev. B* **101**, 241411(R) (2020).
- [25] A. Ott, R. Messina, P. Ben-Abdallah, and S.-A. Biehs, *Appl. Phys. Lett.* **114**, 163105 (2019).
- [26] M. Krüger, T. Emig, and M. Kardar, *Phys. Rev. Lett.* **106**, 210404 (2011).
- [27] M. Krüger, G. Bimonte, T. Emig, and M. Kardar, *Phys. Rev. B* **86**, 115423 (2012).
- [28] F. Herz and S.-A. Biehs, *Europhys. Lett.* **127**, 44001 (2019).
- [29] C. Caloz, A. Alu, S. Tretyakov, D. Sounas, K. Achouri, and Z.-L. Deck-Leger, *Phys. Rev. Appl.* **10**, 047001 (2018).
- [30] C. W. Peterson, W. A. Benalcazar, M. Lin, T. L. Hughes, and G. Bahl, *Phys. Rev. Lett.* **123**, 063901 (2019).
- [31] L. Yuan, Q. Lin, M. Xiao, and S. Fan, *Optica* **5**, 1396 (2018).
- [32] L. D. Tzuang, K. Fang, P. Nussenzeveg, S. Fan, and M. Lipson, *Nat. Photonics* **8**, 701 (2014).
- [33] K. Fang, Z. Yu, and S. Fan, *Phys. Rev. Lett.* **108**, 153901 (2012).
- [34] P. J. van Zwol, L. Ranno, and J. Chevrier, *Phys. Rev. Lett.* **108**, 234301 (2012).
- [35] K. Ito, K. Nishikawa, A. Miura, H. Toshiyoshi, and H. Iizuka, *Nano Lett.* **17**, 4347 (2017).
- [36] J. Kou and A. J. Minnich, *Opt. Exp.* **26**, A730 (2018).
- [37] N. H. Thomas, M. C. Sherrott, J. Broulliet, H. A. Atwater, and A. J. Minnich, *Nano Lett.* **19**, 3898 (2019).
- [38] I. Latella, R. Messina, J. M. Rubi, and P. Ben-Abdallah, *Phys. Rev. Lett.* **121**, 023903 (2018).
- [39] R. M. Abraham Ekeroth, P. Ben-Abdallah, J. C. Cuevas, and A. Garcia Martin, *ACS Photonics* **5**, 705 (2017).
- [40] R. Messina, A. Ott, C. Kathmann, S.-A. Biehs, and P. Ben-Abdallah, *Phys. Rev. B* **103**, 115440 (2021).
- [41] L. J. Fernandez-Alcazar, R. Kononchuk, H. Li, and T. Kottos, *Phys. Rev. Lett.* **126**, 204101 (2021).
- [42] K. Y. Fong, H.-K. Li, R. Zhao, S. Yang, Y. Wang, and X. Zhang, *Nature (London)* **576**, 243 (2020).
- [43] S.-A. Biehs and G. S. Agarwal, *J. Opt. Soc. Am. B* **30**, 700 (2013).
- [44] G. Barton, *J. Stat. Phys.* **165**, 1153 (2016).
- [45] K. Sasihithlu and G. S. Agarwal, *Nanophotonics* **7**, 1581 (2018).
- [46] G. De Chiara, G. Landi, A. Hewgill, B. Reid, A. Ferraro, A. J. Roncaglia, and M. Antezza, *New J. Phys.* **20**, 113024 (2018).
- [47] G. S. Agarwal, *Quantum Optics* (Cambridge University Press, Cambridge, England, 2012).
- [48] See Supplemental Material at <http://link.aps.org/supplemental/10.1103/PhysRevLett.130.110401> for a derivation of the master and Langevin equations, implementation of the Floquet-Shirley approach, definition of the spectra, definition of the heat flux, proof of reciprocity of the heat flux, identifications for coupling parameters for the graphene flakes and Casimir force coupled membranes, and a generalization beyond the white noise assumption.
- [49] S. Thongrattanasiri, F. H. L. Koppens, and F. J. G. de Abajo, *Phys. Rev. Lett.* **108**, 047401 (2012).
- [50] P. J. van Zwol, S. Thiele, C. Berger, W. A. de Heer, and J. Chevrier, *Phys. Rev. Lett.* **109**, 264301 (2012).
- [51] I. Katayama, K. Inoue, Y. Arashida, Y. Wu, H. Yang, T. Inoue, S. Chiashi, S. Maruyama, T. Nagao, M. Kitajima, and J. Takeda, *Phys. Rev. B* **101**, 245408 (2020).
- [52] S. Wu, J. Sheng, X. Zhang, Y. Wu, and H. Wu, *AIP Adv.* **8**, 015209 (2018).